Shock-Associated Noise in Supersonic Jets

S. P. Pao* and J. M. Seiner*
NASA Langley Research Center, Hampton, Virginia

This paper examines the fundamental mechanism of broadband shock noise in an improperly expanded supersonic jet. The study includes circular convergent and convergent-divergent nozzles. The main source of shock noise is determined to be the transient interaction between the shock front and the convected vorticity within the jet plume. The discussion of the noise generation mechanism is based on detailed numerical analysis, theoretical modeling, refined measurements of the jet mean flow, shock-cell structure, turbulence, and noise. Results in this study provide a broad-based generalization for the Harper-Bourne and Fisher analysis and prediction method.

Introduction

EXISTING methods of shock noise prediction may be traced directly to the original investigation of Harper-Bourne and Fisher,[1] in which many of the important aspects of broadband shock noise generation were explored. Familiar results include the scaling of the shock noise intensity with β^4, where

$$\beta = (M_0^2 - 1)^{1/2}$$

and M_0 is the fully expanded jet Mach number, the scaling of the spectral peak frequency with shock-cell length, and the correlated nature of shock noise emission from consecutive shock cells.

Advanced-design jet engines for supersonic and subsonic aircraft may operate at supercritical nozzle pressure ratios. Broadband shock noise from these engines is an important factor in community noise, aircraft interior noise, and structural fatigue. Single and coaxial convergent-divergent (C-D) nozzles are often considered as design options for controlling shock noise. An accurate shock noise prediction method which has the flexibility to cover such variations in exhaust nozzle geometry is essential. An extension of the Harper-Bourne and Fisher theory, as well as the broadening of the experimental data base, has become necessary.

The goal of this coordinated theoretical and experimental research effort is to establish a generalized shock noise prediction method by relating quantitatively the broadband shock noise characteristics to the aerodynamic parameters of the jet exhaust flow. The acoustic and aerodynamic properties of several designs of convergent-divergent nozzles were investigated. The multiple design Mach number approach in this study has made possible a clear understanding of the mechanisms underlying broadband shock noise generation. Earlier results of this investigation have been reported by Seiner,[2,3] Norum,[4] and Pao and Salas.[5] In this paper, a dynamic model of shock noise radiation is proposed which links the shock noise characteristics directly to the aerodynamics of the supersonic jet flow. This model is constructed on the basis of the accumulated theoretical and experimental evidence. It contains the necessary scaling laws to establish a practical shock noise prediction method. It is also intended to provide an accurate description of the physics of shock noise production. The fundamental principles of shock noise generation should be common to jet exhaust flow in the supersonic range regardless of the details of the nozzle geometry. Hence, further developments in shock noise theory or prediction methods can be based upon this model. The remainder of this paper will describe the broadband shock noise model and a critical evaluation of the model by means of experimental data.

Presented as Paper 81-1973 at the AIAA 7th Aeroacoustics Conference, Palo Alto, Calif., Oct. 5-7, 1981; submitted Oct. 22, 1981; revision received Sept. 28, 1982. This paper is declared a work of the U.S. Government and therefore is in the public domain.

*Research Engineer, Aeroacoustics Branch, ANRD. Member AIAA.

The Dynamics of Shock Noise Generation

A typical configuration of a shock containing supersonic jet is shown in Fig. 1. In an improperly expanded supersonic jet, the static pressure of the flow at the nozzle exit is different from the ambient pressure. This pressure difference causes a shock system to form in the jet exhaust plume. The strength and geometry of this shock system is deterministic. It is governed by the design pressure ratio of the nozzle and the operating pressure ratio of the jet. Along the boundary of the jet, a turbulent shear layer develops. According to the experimental results of Ref. 4, the development of this turbulent shear layer is not influenced significantly by the pressure of the shock system. A sonic line for the flow velocity profile is located within the shear layer, and the embedded shock system in the jet plume will not extend beyond this line. A shock cell is defined as a segment of the jet plume between two consecutive intersections between a shock and the sonic line. The first shock cell begins at the lip of the nozzle exit. The shock surface contained within each shock cell has, in general, two conical segments with a single point in common at the axis of the jet. In some cases, a shock disk is formed at the intersection of the conical segments.

Based on recent experimental and theoretical results, it is possible to construct a model which relates the shock noise emission process to the local supersonic flow dynamics. The key assumption in this model is that the broadband shock noise is produced through the interaction between the velocity fluctuations of the turbulent shear layer and the downstream-opening conical segment of the shock surface within each shock cell. The global kinematics of shock noise production, such as the correlated noise emission among consecutive shock cells, is compatible with the Harper-Bourne and Fisher theory. In spite of its simplicity, this model accounts for many of the unique characteristics of broadband shock noise.

The velocity fluctuations in a shear layer can be identified with the vorticity components of the turbulence. The dynamics of shock-vortex interaction in a two-dimensional domain has been discussed in detail by Pao and Salas.[5] Some of the qualitative features of the interaction which are relevant to the construction of the present model are summarized below.

A typical computed result for shock-vortex interaction is shown in Fig. 2. A simple clockwise-rotating vortex embedded in the supersonic freestream is convected through a shock front from left to right. The interaction between the shock and the vortex creates a complex pressure pattern behind the shock. In Fig. 2, the pressure contours are normalized with

respect to the unperturbed pressure downstream of the shock. The center of the vortex is shown as a deep pressure depression with its center marked with a cross. A cylindrical acoustic wave front propagating outward from the center of the vortex can be recognized by its imposition of a sharp curvature on a set of originally smooth pressure contour lines. The location of the wave front is indicated by a circle with dashed lines. Since the mean flow velocity behind the shock front is moving subsonically relative to the shock, the cylindrical wave front intersects with the shock. The acoustic wave amplitude varies around the cylindrical front. Both the maximum and the minimum pressure amplitude occur at the intersections between the acoustic wave front and the shock. Of particular interest is the amplitude and size of the high-pressure region, which is marked by the letter H in Fig. 2. For a combination of shock strength and vorticity typical of a supersonic exhaust plume, the pressure amplitude at the maximum, marked by P in Fig. 2, can reach 20% of the unperturbed ambient pressure behind the shock. The size of this pressure spot is much smaller than the size of the vortex core.

A linear analysis[5] of this noise emission process during shock-vortex interaction explains the mechanism through which the high-pressure spot is formed. As far as acoustic radiation is concerned, the vortex-induced velocity field in the supersonic freestream can be considered as an acoustic source distribution which is activated only at its intersection with the shock front. This distribution has a quadrupole directivity pattern and a source strength proportional to d^{-2}, where d is the distance from the center of the vortex. The source strength vanishes within the solidly rotating vortex core. Since the noise radiation process occurs at the intersection of the shock and the moving vortex, and the vortex is moving away downstream from the shock at a subsonic speed, there is a path of coincidence along which the high-amplitude pressure spot is formed, Fig. 3. Since the strongest source region is concentrated around the vortex core, the width of the pressure spot is much narrower than the size of the vortex core.

The kinematics of a vortex interacting with a normal shock can be transposed to the situation in which the vortex interacts with an oblique shock. A sketch is shown in Fig. 4 for the typical geometry of shock-vortex interaction in a jet. A vortex convected at supersonic speed is shown passing through the downstream facing conical segment of the shock front. After interacting with the shock, the vortex continues to move downstream at a lower supersonic speed. The radiated acoustic wave front is expanding and also convected in a direction parallel to the shock front. The segments of the acoustic wave front with the highest intensity move outward along the shock, into the subsonic portion of the shear layer, and finally into the far field. The interaction between a vortex and the upstream facing conical segment of the shock surface can also generate noise. However, the acoustic wave front thus generated will initially move toward the centerline of the jet and then be swept into the next downstream-facing conical shock front.

Several points of immediate significance should be mentioned here. The dynamics of shock-vortex interaction in both a two-dimensional and a three-dimensional flow are qualitatively similar, except for the known differences for wave propagation in odd and even dimensional spaces. If a mathematical model for the vortex is chosen differently from the one given in Ref. 5, the details of the acoustic pressure distribution will be different. However, the essential features of shock-vortex interaction, such as the formation of a high pressure spot, should remain unchanged.

It was shown in Pao and Salas[5] that the amplitude of noise emitted through the shock-vortex interaction process is proportional to the first power of the fluctuating velocity components. This result is in good agreement with the observed pre-eminance of shock noise in the forward arc direction near a supersonic jet. Theoretically, the jet mixing noise amplitude is proportional to the second power of the amplitude of the fluctuating velocity components. Hence, based upon the source strength order of magnitude, the shock-associated noise is expected to dominate over the

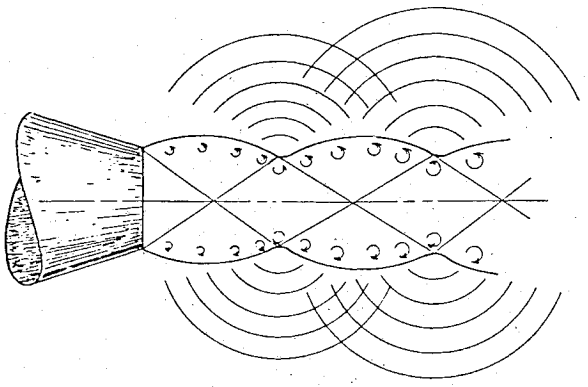

Fig. 1 Shock-associated noise.

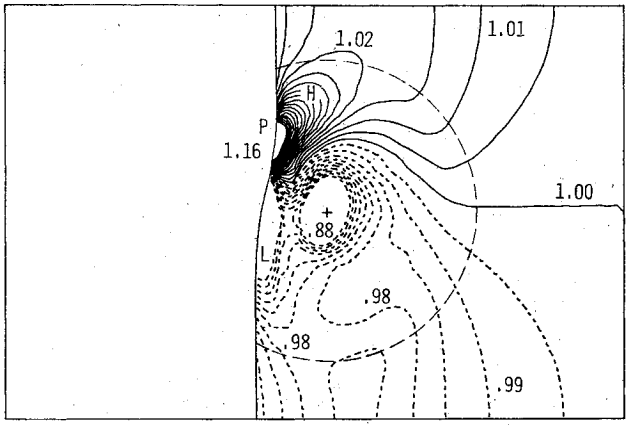

Fig. 2 Typical computed pressure contours for shock-vortex interaction in two dimensions.

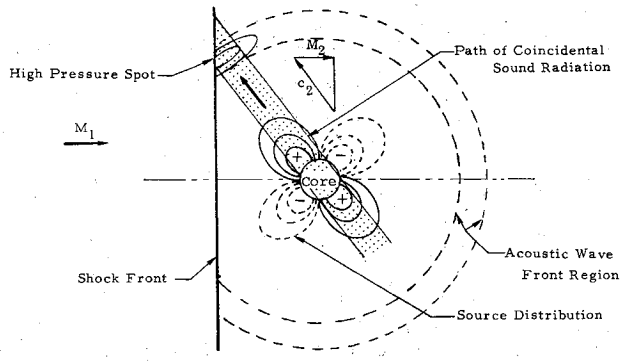

Fig. 3 The path of coincidental sound radiation and the formation of the high pressure spot on the acoustic wave front.

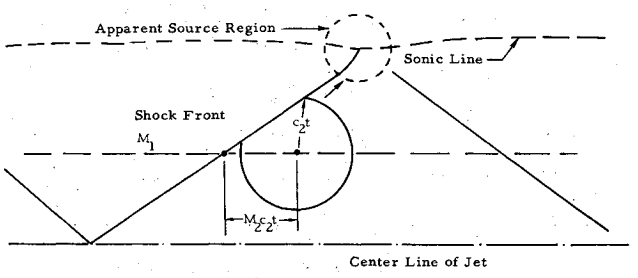

Fig. 4 Sound source location.

mixing noise in the forward arc where the convective amplification factor for mixing noise is small.

Another significant conclusion can be deduced from the process through which the high-amplitude pressure spot on the acoustic front is formed. Let the tangential velocity at the rim of the vortex core remain constant, while the size of the vortex core varies. According to Fig. 3, the region of coincidental radiation increases linearly with the size of the vortex. Since the source intensity distribution is similar for all sizes of the vortex, the final amplitude and the width of the high-pressure spot are proportional to the size of the vortex. For a fixed amount of total vorticity, more shock-vortex interaction noise will be radiated if all of the vorticity is concentrated in a large vortex than if the vorticity is randomly distributed among a number of smaller vortices. This is a familiar result in random signal analysis where the intensity, instead of the amplitude, of the individual random components is summable. Hence, this interaction model favors the production of low-frequency shock noise. If the vorticity components in the turbulent shear layer have flat distributions in wavenumber space, then the expected sound power production efficiency is proportional to k^{-2}, where k is the wavenumber for the vorticity.

In the analysis of Pao and Salas,[5] the intensity of the acoustic wave has no explicit dependence on temperature. This result corresponds to the observed experimental data that shock noise intensity is temperature-independent.

Broadband Shock Noise Spectrum

One of the most striking features of shock noise is that the spectral shape is almost invariant with respect to the direction of radiation and the overall amplitude of the shock noise. In general, the acoustic spectral density function decays at the slow rate of ω^{-2} or ω^{-3} in the high-frequency limit, where ω is the circular frequency. In the frequency range below the peak frequency, the spectral density level rises very steeply with ω at a rate of ω^4 or higher (Fig. 5). In this section, some classical results of time series analysis will be employed to assess the physical significance of such a peculiar spectral distribution.

For a given time-series signal which can be either random or deterministic, the corresponding power spectral density can be obtained from the autocorrelation function $R(\tau)$:

$$S(\omega) = \frac{1}{\pi}\int_0^\infty R(\tau)\cos\omega\tau\,d\tau \tag{1}$$

where $S(\omega)$ is the power spectral density function, and the cosine transformation is used because $R(\tau)$ is symmetrical with respect to τ. In the high-frequency limit, a repeated integration by parts of Eq. (1) results in a series in ω^{-2} for $S(\omega)$:

$$S(\omega) = \frac{1}{\pi}\{R(0)\omega^{-2} - R'''(0)\omega^{-4} + \ldots\} \tag{2}$$

First of all, Eq. (2) states that the high frequency behavior of $S(\omega)$ is governed by the behavior of $R(\tau)$ near its origin. Second, in order for the function $S(\omega)$ to decay at a rate of slower than ω^{-4} in the high-frequency limit, the coefficient $R'(0)$ must be nonzero. In this regard, it is necessary to examine the definition of the autocorrelation function itself:

$$R(\tau) = E\{f(t)f(t+\tau)\} \tag{3}$$

where $f(t)$ is a stationary random function, and E is the notation for the ensemble averaged value.[6] For a differentiable $f(t)$, a theorem in Ref. 6 states that $R(\tau)$ will be at least twice differentiable. Since $R(\tau)$ is symmetrical with respect to and differentiable at $\tau=0$, $R'(0)=0$. There are stationary random processes for which $R'(0)$ is nonzero. A random sequence of square waves is such an example. For this

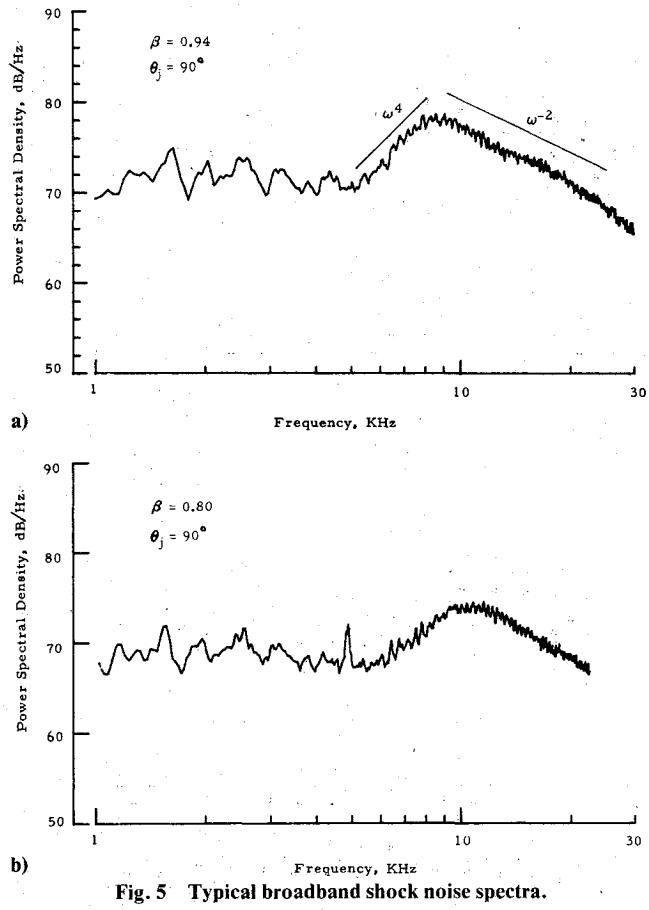

Fig. 5 Typical broadband shock noise spectra.

class of stationary random processes, $f(t)$ must contain finite discontinuities.

In the case of broadband shock noise, the spectral behavior in the high-frequency range implies that the source function is impulsive. The formation of the high-pressure spot in the shock-vortex interaction process may be responsible for it.

The low-frequency spectral behavior can also be obtained from Eq. (1) in terms of a power series of ω^2 if $\cos\omega\tau$ is replaced by its power series form:

$$S(\omega) = \frac{1}{\pi}\int_0^\infty R(\tau)\,d\tau - \frac{\omega^2}{2\pi}\int_0^\infty \tau^2 R(\tau)\,d\tau + \frac{\omega^4}{4!\pi}\int_0^\infty \tau^4 R(\tau)\,d\tau \ldots \tag{4}$$

In order that the low-frequency portion of the spectral density function will follow a ω^4 dependence, the coefficients of the first two terms in Eq. (4) must vanish:

$$\int_0^\infty R(\tau)\,d\tau = 0 \tag{5a}$$

$$\int_0^\infty \tau^2 R(\tau)\,d\tau = 0 \tag{5b}$$

In other words, both the total area under the correlation function and its second moment must vanish. Experimental shock noise data indicate that the typical wavelength at the peak of the spectrum equals the length of the shock cell. If the radiated noise is correlated only within a single shock cell, an ensemble-averaged time signature of the shock noise signal will be similar to the sketch shown in Fig. 6a. However, such a time signature will lead to an autocorrelation function with a single positive lobe and a single negative lobe, as shown in

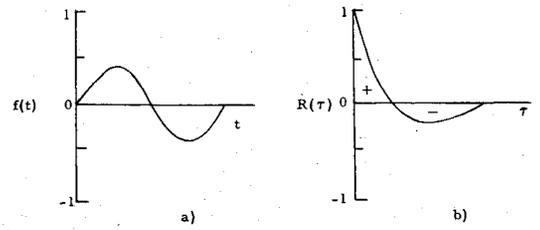

Fig. 6 A hypothetical ensemble-averaged time history and its corresponding correlation function.

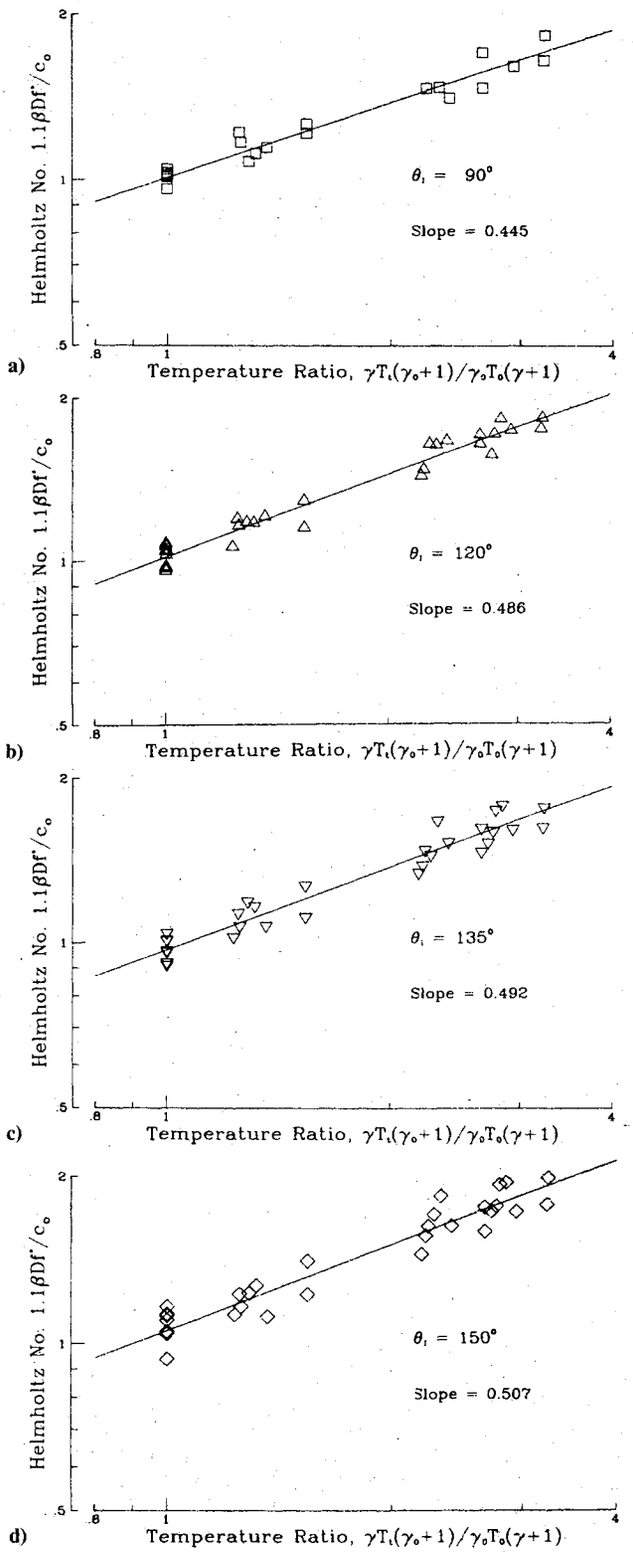

Fig. 7 Correlation of the shock noise peak frequency with the temperature ratio.

Fig. 6b. When the positive and the negative areas are equal, Eq. (5a) is satisfied. However, Eq. (5b) cannot be satisfied simultaneously because the second moment of the negative area in Fig. 6b is obviously larger than the second moment of the positive area. This exercise demonstrates that the radiated acoustic signal must repeat itself more than one single positive and negative cycle in order to achieve a steep rise in the low-frequency domain. There are several physical mechanisms which will be able to satisfy this mathematical requirement. The vorticity in the turbulent mixing layer may correlate over several shock cell lengths. This is certainly possible for low β jets where the shock cell spacing is small. While this explanation may not hold for jets with long shock cells, another mechanism is possible. After the passage of a large vortex through the first shock cell, an induced motion can be set up for the entire chain of shock cells. The transient motion of the shock cells can radiate a component of low-frequency noise. Furthermore, this component of low-frequency noise may have the appearance of a screech tone. It is quite plausible because the observed broadband shock noise spectrum is often bounded at the low-frequency end by a screech tone. A third mechanism is yet possible. Even if the jet contains only one or two shock cells, the position of the shock cell can oscillate according to a natural jet column mode. The resulting low-frequency noise radiation will again provide a sharp low-frequency cutoff for the broadband shock noise spectrum.

It can be concluded that the shape of the spectrum alone can reveal some important physical requirements of shock noise generation. The high-frequency behavior of the spectrum shows that the source of shock noise is highly impulsive in nature. The sharp cutoff in the low-frequency range implies a number of plausible physical mechanisms, including a possible link between broadband shock noise and the screech tones.

Peak Frequency Scaling Laws

The scaling laws for the peak frequency of the broadband shock noise have been re-examined by Norum and Seiner[4] in light of their experimental data. The peak frequency can be correlated on either a Helmholtz or a Strouhal number basis. The definition of these two numbers are given as follows:

$$Hm = f_p \bar{L}/c_0 \tag{6}$$

$$St = f_p \bar{L}/U_c \tag{7}$$

The average shock cell spacing $\bar{L}$ is used in both cases as the reference length. The ambient speed of sound c_0 is used as the characteristic speed for the Helmholtz number, while the eddy convection velocity in the turbulent shear layer U_c is chosen for the Strouhal number. The data in Norum and Seiner[4] included peak frequency measurements of shock noise from jets issuing from convergent nozzles as well as convergent-divergent nozzles of two different design Mach numbers. It was shown, from the acoustic data measured at 90 deg from the axis of the jet, that the Helmholtz number remains constant for all values for β while the Strouhal number changes significantly over the same range of values for β. Therefore, the Helmholtz number appears to be a more versatile empirical parameter for the correlation of shock noise peak frequency. This conclusion may differ from other analyses in the literature; yet it is derived directly from experimental data over a wide range of test conditions. It is an objective result and should be considered on its own merit.

The peak frequency of shock noise radiated in other directions, f_p, is related to the peak frequency at 90 deg by means of a Doppler shift factor based upon the convection velocity, U_c:

$$f_p = f^*/(1 - M_c \cos\theta_j) \tag{8}$$

where f^* is the peak frequency at 90 deg, θ_j is the angle from the axis of the jet, and M_c is the convection Mach number given by U_c divided by c_0. This convection factor is part of the original model of Harper-Bourne and Fisher[1] and the same conclusion has been reached from analyzing the data as obtained in the present study.

By using the Helmholtz number and the convective Doppler shift factor as a starting point, an attempt is made to investigate the behavior of the peak shock noise frequency in both cold and heated jets. The most comprehensive data set of shock noise in heated circular jets is given by Tanna.[7] By combining Eqs. (6) and (8), a modified Helmholtz number can be defined as:

$$H_1 = 1.1\beta D f_p (1 - M_c \cos\theta_j)/c_0 \tag{9}$$

In this equation, the average shock cell spacing has been replaced by $1.1\beta D$, and the convection velocity is chosen to be $0.7U_j$, where U_j is the expected jet velocity at full expansion.

The data set in Tanna[7] covers a wide range of values in β and T_t, the stagnation temperature of the heated jet. The ratio of specific heats for these heated jets is not a constant; it ranges from 1.33 to 1.40. There are a total of 40 run conditions. The shock nose peak frequency can be determined at five different angles of noise emission in most of the runs. All of the available shock noise peak frequency data in Tanna[7] are used in the present correlation study.

The Helmholtz number as defined by Eq. (9) is correlated with a modified temperature ratio $\gamma(1+\gamma_0)T_t/\gamma_0(1+\gamma)T_0$. The results are shown in Figs. 7a-d. A first-order least-square fit has been obtained for each group of data points. The slope of the least-square fit indicates that the Helmholtz number for the heated jets is proportional to

$$\{\gamma(1+\gamma_0)T_t/\gamma_0(1+\gamma)T_0\}^{0.5}$$

This correlation has a significant physical meaning. For each given stagnation temperature of the jet plume, there is a uniquely defined critical speed of sound:

$$c^* = \{2\gamma RT_t/(\gamma+1)\}^{1/2} \tag{10}$$

where R is the gas constant. If the value of c_0 in the definition of the Helmholtz number, Eq. (9), is replaced by the corresponding critical speed of sound for an unheated jet, namely

$$c_0^* = \{2\gamma_0 RT_0/(\gamma_0+1)\}^{1/2} \tag{11}$$

then the value of the Helmholtz number will be changed by only a constant factor. In this case, a generalized Helmholtz number can be defined:

$$H^* = \frac{1.1\beta D f_p (1 - M_c\cos\theta_j)}{c_0^*}\left\{\frac{\gamma(1+\gamma_0)T_0}{\gamma_0(1+\gamma)T_0}\right\}^{1/2}$$

$$= 1.1\beta D f_p (1 - M_c\cos\theta_j)/c^* \tag{12}$$

Following the correlation in the above discussion, H^* is a constant (Fig. 8). This is a simple, yet highly significant result. The peak frequency of the shock noise is now related entirely to physical quantities in the jet flow by means of Eq. (12). In the previous definitions of the Helmholtz number, the ambient speed of sound is a quantity external to the jet flow.

However, a mystery remains in Eq. (12). The shock noise peak frequency scales with not one but two characteristic velocities: c^* and U_c. A plausible explanation can be obtained by using the shock vortex interaction model. Referring to the sketch given in Fig. 9, one can see that the vortex is convected toward the oblique shock front at a supersonic Mach number of M_1. However, the effective Mach number of the oblique shock is the component of M_1 in a direction normal to the shock front, M_n. The acoustic production process for the shock vortex interaction is governed by M_n. For all of the data obtained in the present investigation (with values of β ranging from 0.4 to 2.1) the value of M_n is less than 1.3. The higher values of M_n are normally associated with jets with higher β values. As an approximation, the convection velocity corresponding to M_n is very close to c^*.

The explanation for the Doppler shift effect on the shock noise peak frequency is different for the low and the high β ranges. In the low β cases, the shock cell spacing is small and the vortex can pass through the shock cell system at the convection speed in the jet mixing layer. The acoustic radiation at the corners of the shock cells are phase related through this convection velocity. The Doppler shift effect in the far field is obtained by the Harper-Bourne and Fisher theory. In the high β range, say $\beta > 1$, the physical picture is different. The shock cell length is now greater than the jet diameter. The turbulence measurements of Seiner and

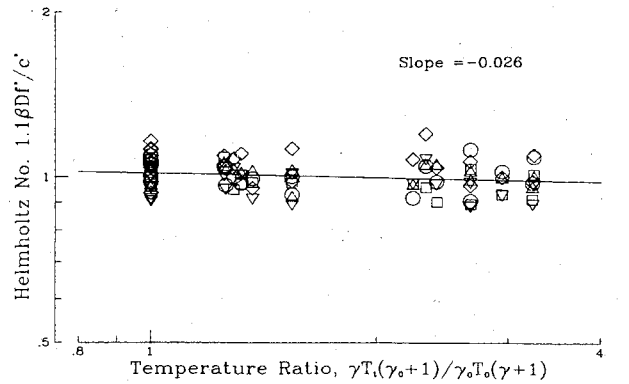

Fig. 8 Correlation of a generalized Helmholtz number for broadband shock noise peak frequency with the temperature ratio.

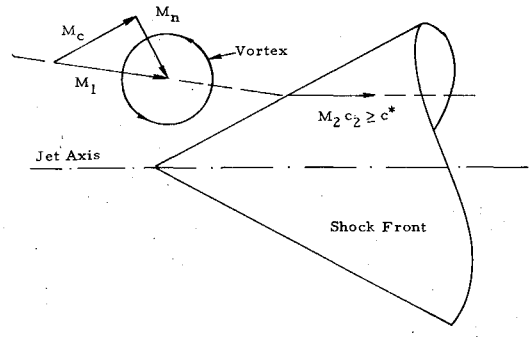

Fig. 9 Relations between the oblique shock cone, effective Mach number, and convection velocity.

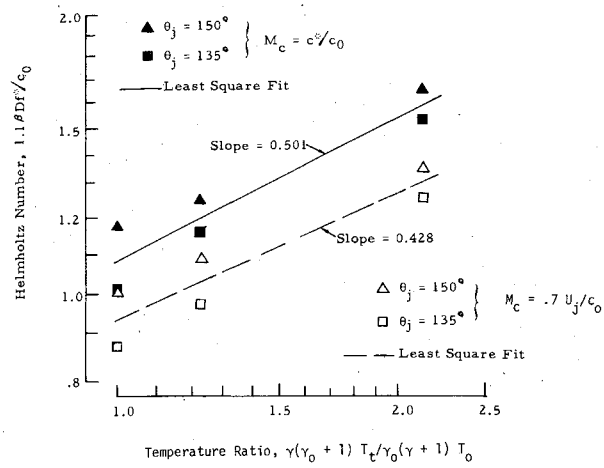

Fig. 10 Effects of different convection velocity assumption for $\beta = 0.40$, $M_j = 1.077$.

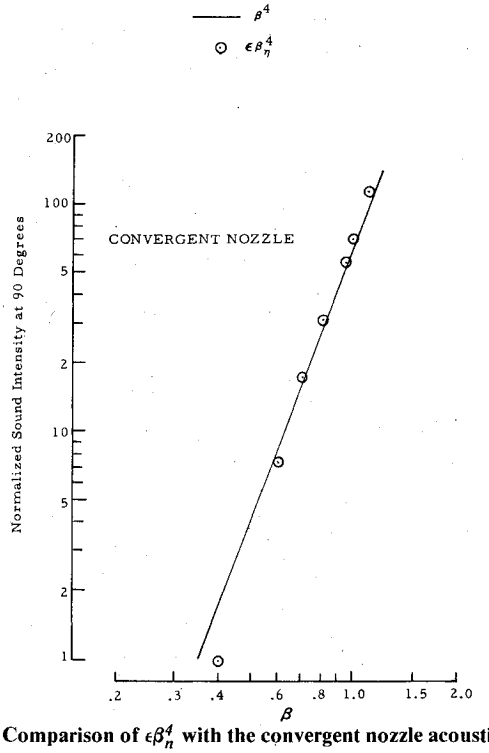

Fig. 11 Comparison of $\epsilon\beta_n^4$ with the convergent nozzle acoustic data, β^4.

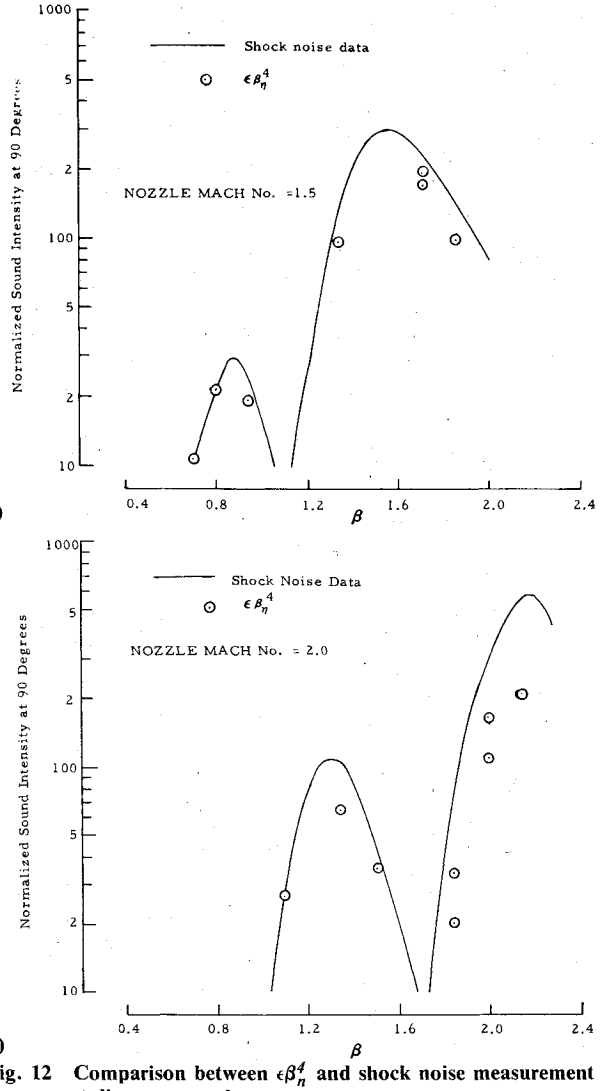

Fig. 12 Comparison between $\epsilon\beta_n^4$ and shock noise measurement of convergent-divergent nozzles.

Norum[3] indicate that the turbulence structure in a shock containing jet is not significantly different from the corresponding turbulence structure in a shock-free mixing layer. Thus, the expected turbulence correlation length is on the order of one or two jet diameters. Correlated noise emission over several shock cells is quite unlikely. On the other hand, acoustic measurements of the broadband shock noise in the near field by Seiner and Yu[8] shows that Doppler shift is observed in the near field of an individual shock cell. The illustration in Fig. 8 shows that the Doppler shift of the broadband shock noise can indeed occur for a single shock cell. There is a convective velocity component, M_c, parallel to the shock front during the interaction between a vortex and an oblique shock. The magnitude of this convective velocity is significant for $\beta > 1$. In such cases, the oblique shock is inclined at less than 45 deg from the jet axis and the convection velocity is greater than $0.7U_j$. This appears to be a natural extension of the Harper-Bourne and Fisher theory. Following this shock-vortex interaction model, it is physically possible for the shock noise to be produced according to a characteristic velocity of c^*, while the far-field Doppler effect appears to follow a different characteristic velocity, U_c.

Another interesting result concerning the convective Doppler factor follows as a consequence of the shock-vortex interaction model. In order that the shock cell structure can repeat itself, the convection Mach number downstream of the oblique shock front has to be supersonic. Therefore, the minimum convection velocity for the shock noise is the critical speed of sound, c^*. For supercritical jets with a low β value, the convection velocity as defined by $0.7U_j$ can fall below c^* by a substantial amount. In the above analysis for the peak shock noise frequency, some irregularities have been observed if one tries to extract the temperature correlation exponent from run conditions with low β values. This point is illustrated in Fig. 10. However, if a minimum value of c^* is imposed on the definition of U_c, the temperature correlation exponent is restored to a value close to 0.5.

Shock Noise Intensity

The determination of shock noise intensity for supersonic jets emanating from convergent-divergent nozzles at off-design operating conditions is a major objective of this investigation because the results of Harper-Bourne and Fisher cannot be immediately extended. However, computing shock noise intensity from first principles is difficult. According to the shock-vortex interaction model, the shock noise intensity depends on the intensity of the vorticity components of the turbulence, the strength of the oblique shock, the area of interaction, and the dynamic process of interaction. Although such a computational process appears feasible based upon the numerical study of Pao and Salas,[5] a substantial amount of research remains to be done. In this section, an empirical correlation between the measured shock noise intensity and a typical shock-cell strength will be discussed.

The reasoning for the empirical correlation contains two steps. First, an attempt can be made to correlate the shock noise intensity for choked jets with the oblique shock strength in the jet flow. Second, the aerodynamic measurements have shown that the turbulence in the mixing layer is not altered significantly by the oblique shock system. It should remain the same for jets coming from either a convergent nozzle or a C-D nozzle as long as the β value remains the same. Hence, it stands to reason from the shock-vortex interaction model that the shock noise intensity is proportional to the strength of the oblique shock at a fixed value of β. For this empirical correlation, a new parameter β_n is defined as

$$\beta_n = (M_n^2 - 1)^{1/2} \tag{13}$$

where M_n is the effective Mach number for the downstream facing shock cone. Since the shock intensity varies along the

shock cone, a typical value near the center of the shear layer in the second shock cell is chosen. Extensive measurements of the shock strength have been obtained for the convergent nozzle, the $M = 1.5$ nozzle, and the $M \doteq 2.0$ nozzle.

From an intuitive standpoint, the shock intensity can be assumed to follow β_n. This hypothesis can be tested against the acoustic data. The results for the convergent nozzle are shown in Fig. 11. An arbitrary constant factor ϵ is chosen such that the prediction and the experimental acoustic data matches at a single point. From the good agreement between the prediction and the experimental data, one can state that the present hypothesis agrees with the scaling law of Harper-Bourne and Fisher,

$$\alpha_0 \beta^4 = \epsilon \beta_n^4 \tag{14}$$

where α_0 is the scaling constant in the original Harper-Bourne and Fisher shock noise model. Furthermore, one is encouraged to test the $\epsilon\beta_n^4$ scaling law against the data sets for the C-D nozzles without changing the scaling constant, ϵ.

The comparison for the C-D nozzles is shown in Fig. 12. Although the absolute level of the prediction of the shock noise intensity at various β values differs by as much as 3 dB from the experimental data, the trends are similar. This result is quite encouraging because it demonstrates that the shock noise intensity can be related to the local aerodynamic quantities in a shock containing jet plume.

As pointed out previously by Norum and Seiner,[4] the detailed acoustic measurements of the shock noise indicate that the shock noise intensity is not necessarily omnidirectional. Both the source directivity and the Doppler shift effect may contribute to the far-field directivity. Further analysis will be required for a better understanding of the contributing factors of shock noise directivity.

Concluding Remarks

A self-consistent model of shock noise generation has been established in the present paper. The key noise generation mechanism is assumed to be the interaction between the vorticity in the turbulent mixing layer and the shock system in the jet. The shock noise amplitude is proportional to the first power of the fluctuating velocity components in the turbulence of the mixing layer. Theoretically, this first-order dependence on the fluctuating velocity is powerful enough for the shock noise to dominate over the mixing noise in the forward arc directions. The typical shapes of the shock noise spectrum imply that the origin of shock noise is highly impulsive, and the source signal can be correlated over many shock cells. The best correlation parameter for shock noise peak frequency is the Helmholtz number based on the average shock cell length and the ambient speed of sound. From an analysis of the dependence of the Helmholtz number on the jet temperature, a generalized definition of the Helmholtz number has been established such that it remains constant for both cold jets and heated jets. A new scaling law for the intensity of broadband shock noise has also been established. It is based on the typical strength of the oblique shock in the jet flow. This scaling law is compatible with the Harper-Bourne and Fisher theory while it is applicable to choked jets from convergent nozzles as well as improperly expanded jets from convergent-divergent nozzles.

In summary, the present model for broadband shock noise is a natural extension to the Harper-Bourne and Fisher theory. In view of the good agreement between the analytical model and the experimental data for single-stream circular jets, the authors believe that the physics of shock noise generation has been modeled correctly. Thus, methods of broadband shock noise prediction can be developed for engine design purposes without having first to obtain an extensive acoustic data base.

References

[1] Harper-Bourne, M. and Fisher, M. J., "The Noise from Shock Waves in Supersonic Jets," AGARD-CP-131, 1973.

[2] Seiner, J. M. and Norum, T. D., "Experiments of Shock Associated Noise on Supersonic Jets," AIAA Paper 79-1526, 1979.

[3] Seiner, J. M. and Norum, T.D., "Aerodynamic Aspects of Shock Containing Jet Plumes," AIAA Paper 80-0965, 1980.

[4] Norum, T. D. and Seiner, J. M., "Location and Propagation of Shock Associated Noise from Supersonic Jets," AIAA Paper 80-0983, 1980.

[5] Pao, S. P. and Salas, M. D., "A Numerical Study of Two-Dimensional Shock Vortex Interaction," AIAA Paper 81-1205, 1981.

[6] Papoulis, A., *Probability, Random Variables and Stochastic Processes*, McGraw-Hill Book Co., New York, N.Y., 1965, pp. 284-318.

[7] Tanna, H. K., Dean, P. D., and Burrin, R. H., "The Generation and Radiation of Supersonic Jet Noise, Vol. 4, Shock Associated Noise Data," Aero-Propulsion Laboratory, Air Force Wright Aeronautical Laboratories, Technical Rept. AFAPL-TR-76-65, 1976.

[8] Seiner, J. M. and Yu, J. C., "Acoustic Near Field and Local Flow Properties Associated with Broadband Shock Noise," AIAA Paper 81-1975, 1981.